

Critical fluctuations and pinning effects on the vortex transport in superconducting Y-Ba-Cu-O single crystals

N.-C. Yeh, W. Jiang, D. S. Reed, and U. Kriplani

Department of Physics, California Institute of Technology, Pasadena, California 91125

F. Holtzberg

IBM Research Division, Thomas J. Watson Research Center, Yorktown Heights, New York 10598

(Received 2 October 1992)

The critical fluctuations and pinning effects in the vortex state of twinned superconducting Y-Ba-Cu-O single crystals are investigated. A second-order vortex-solid melting transition is manifested by the *universal* static and dynamic exponents $\nu \approx \frac{2}{3}$ and $z \approx 3$ and the *universal* vortex-transport functions, independent of the experimental techniques and the magnitude and orientation of the applied magnetic fields. The vortex-correlation length and the critical-relaxation rate are also determined.

The large thermal and disorder fluctuations in the vortex state of high-temperature superconductors (HTS) result in interesting vortex properties which have stimulated intense research effort.¹⁻¹⁷ However, it is still controversial whether the “phase boundary” below the mean-field upper critical field in the vortex phase diagram is a vortex-solid “melting transition,”¹⁻⁵ or an “irreversible line” that defines the onset of vortex “depinning.”⁶⁻⁸ Although a first-order vortex-solid melting transition may exist in untwinned, clean-limit single crystals,⁹ a second-order melting transition should be common in most samples with moderate disorder. Such a second-order phase transition, if it exists, should be manifested by *universal* static and dynamic critical exponents which are *independent* of the sample, experimental technique, magnitude, and orientation of the applied magnetic field. However, the large errors in the previously reported critical exponents^{10,11} are either an indication of the lack of universality (thereby implying no phase transition), or a suggestion of additional complications (such as possible pinning of the vortex liquid by the twin boundaries after the vortex-solid melting transition), which may have hindered decisive experimental interpretations. In this Brief Report, we address these issues by demonstrating *universal* critical exponents and *universal* vortex-transport functions in twinned Y-Ba-Cu-O single crystals. The universality is shown by the independence of two different types of experimental techniques over two decades of dc magnetic fields (H) and for two field orientations ($H_{\parallel c}$ and $H_{\perp c}$). In addition, the vortex-correlation length and the critical-relaxation rate are determined. We also show quantitatively how finite-size effects such as the twin boundary pinning influence the vortex critical fluctuations. These effects can explain why previous reports^{10,11} show lack of universality.

The sample studied in this work is a well-characterized twinned Y-Ba-Cu-O single crystal,¹² with 100% superconducting volume from magnetization measurements, zero-field superconducting temperature $T_{c0} = 92.95$ K, normal state resistivity at T_{c0} $55 \mu\Omega$ cm, resistive transi-

tion width < 0.1 K, magnetic transition width < 0.2 K, and average twin boundary separation $\approx 2 \mu\text{m}$ from reflecting-light microscopy. The experiments include measurements of the electric field (E) versus dc current density (J) isotherms for both $H_{\parallel c}$ axis and $H_{\perp c}$ axis, and ac impedance (ρ) and phase (ϕ) versus frequency (ω) isotherms from 10^2 to 10^6 Hz ranging from 0 to 70 kOe. Details of the sample characterizations and experimental techniques are given elsewhere.¹²⁻¹⁶ The single crystal was subsequently irradiated with various doses of 3-MeV protons in order to introduce controlled densities of point defects, and the dc E -vs- J measurements were repeated over nine magnetic fields and for both $H_{\parallel c}$ and $H_{\perp c}$ after each irradiation. Since the vortex critical fluctuations after proton irradiations follow the same universal scaling behavior and are given elsewhere,¹⁶ we only focus below on the results and analysis of the transport data before irradiations.

In the weak pinning limit and near a second-order vortex-solid melting transition, the temperature deviations from the melting temperature $T_M(H)$ in a constant magnetic field H , as well as the applied current density J , drive the vortex system away from the critical point. The critical scaling hypothesis suggests the form for the vortex-correlation length,¹⁸

$$\xi(T, H, J) = \xi_0(H) |1 - (T/T_M)|^{-\nu} f(x), \quad x \equiv \frac{J}{J_T(T, H)}, \quad (1)$$

where J_T , the characteristic “scaling” current for the crossover between current and temperature-dominated regimes, is given by

$$J_T(T, H) = \frac{k_B T}{\Phi_0 [\xi_0(H) |1 - (T/T_M)|^{-\nu}]^{(d-1)}}, \quad (2)$$

where d is the dimensionality, Φ_0 is the flux quantum, ξ_0 is the zero-temperature correlation length, ν is the static exponent, and $k_B T$ is the thermal energy. The functional

form of $f(x)$ satisfies two conditions: $f(x) \rightarrow 1$ for $x \rightarrow 0$ and $f(x) \rightarrow x^{-1/(d-1)}$ for $x \rightarrow \infty$, so that Eq. (1) is reduced to the usual expressions $\xi = \xi_0 |1 - (T/T_M)|^{-\nu}$ for $J \ll J_T$, and $\xi = [k_B T / (J \Phi_0)]^{1/(d-1)}$ for $J \gg J_T$.³ The correlation length ξ may be physically interpreted as the average size of the “dislocation loops”,^{1-3,12,13} determined by balancing the vortex-solid elastic and thermal energies for $T < T_M$, and as the size of the short-range vortex order in the vortex-liquid state.^{1,2}

When the applied current density J is comparable to J_T , the electric field (E) due to the vortex dissipation can be written according to the following scaling relation:^{3,12,13}

$$E = J |1 - (T/T_M)|^{\nu(2+z-d)} \tilde{E}_{\pm}(x), \quad (3)$$

where x is defined in Eq. (1), z is the dynamic exponent related to the critical-relaxation rate (ω_T) of the dislocation loops through the expression $\omega_T \propto \xi^{-z}$,^{3,19} and $\tilde{E}_{\pm}(x)$ are universal functions for $T > T_M$ (\tilde{E}_+) and $T < T_M$ (\tilde{E}_-), respectively.^{3,12,13} In Figs. 1(a) and 1(b) we show the E -vs- J isotherms at constant magnetic fields $H(\parallel c) = 3$ kOe and $H(\parallel c) = 30$ kOe, and the insets show the universal functions \tilde{E}_{\pm} obtained by “collapsing” E -vs- J isotherms with the relation $\tilde{E} \equiv (E/J) |1 - (T/T_M)|^{\nu(d-2-z)}$ and $\tilde{J} \equiv (J/T) |1 - (T/T_M)|^{\nu(1-d)}$ [see Eqs. (1) and (3)]. The same analysis for $d=3$ has been applied to data in magnetic fields ranging from 1 to 70 kOe for both $\mathbf{H} \parallel c$ and $\mathbf{H} \perp c$.¹⁵ The universality is manifested by the same critical exponents $\nu = 0.65 \pm 0.05$ and $z = 3.0 \pm 0.2$ for *all* fields in both directions. The melting temperatures [$T_M(H)$] determined from the critical scaling analysis are plotted on the H -vs- T vortex phase diagram in Fig. 2. Note that the anisotropic melting lines $H_{M\parallel c}(T)$ for $\parallel c$ and $\perp c$ follow the temperature dependence $H_M(T) = H_M(0) |1 - (T/T_{c0})|^{2\nu_0}$, where $H_M(0)$ is a constant, and $\nu_0 \approx \frac{2}{3}$ is the zero-field critical exponent, consistent with the 3D XY model.³ The critical regimes of the melting lines are in good agreement with those estimated by using the Ginzburg criterion,²⁰ and are shown by the shaded areas in Fig. 2. We note that accurate critical exponents should be determined from the E -vs- J isotherms within the critical regime. Otherwise, incorrect estimates of ν and z may result from the influence of the mean-field $H_{c2}(T)$ line.^{10,12}

We obtain the vortex-correlation length $\xi_0(H)$ by the following simple procedure: We assume $\tilde{E}_+(x) \approx \tilde{E}_-(x) \approx \tilde{E}_0 x^{(z-1)/2}$ for $x \rightarrow \infty$ and $\tilde{E}_+ \approx \tilde{E}_0$ for $x \rightarrow 0$ [see the inset of Fig. 1(b) and Ref. 3], where \tilde{E}_0 is a constant independent of T and J , $x \equiv (\tilde{J}/\tilde{J}_T) = (J/J_T)$, and $\tilde{J}_T = k_B / (\xi_0^2 \Phi_0)$. Thus, we obtain \tilde{J}_T (and therefore ξ_0) directly from the universal function \tilde{E}_+ . The magnetic-field dependence of $\xi_0(H)$ for $1 \leq H \leq 70$ kOe is depicted in the inset of Fig. 2. We note that ξ_0 increases gradually from ~ 200 to ~ 800 Å with the increasing H , consistent with a stronger intervortex correlation in higher magnetic fields.

Next, we consider finite-size effects such as the twin boundaries in Y-Ba-Cu-O single crystals and the screw dislocations²¹ in Y-Ba-Cu-O epitaxial films. As T approaches $T_M(H)$, the growth of ξ will eventually be dis-

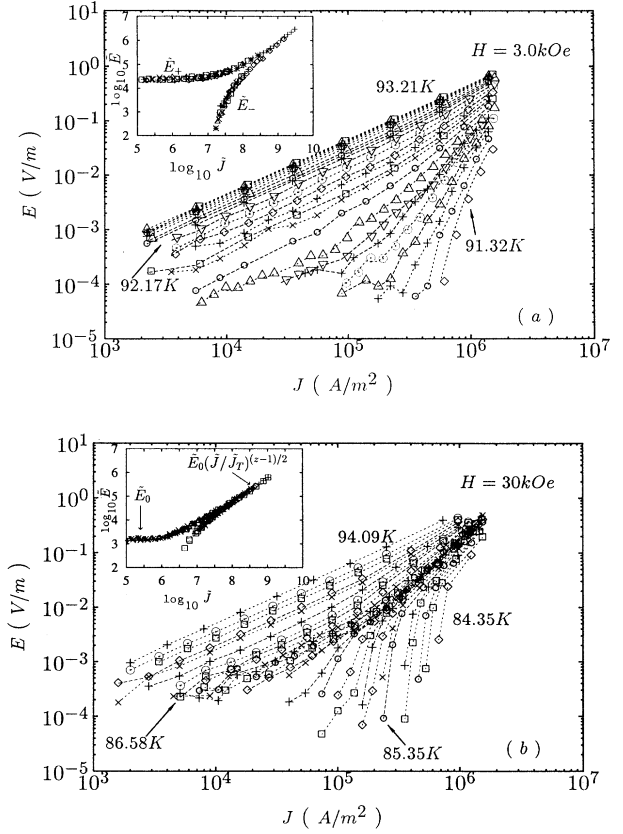


FIG. 1. The electric field (E) vs current density (J) isotherms for $H \parallel c$ axis and (a) $H = 3$ kOe, (b) $H = 30$ kOe. The insets are the universal functions \tilde{E}_{\pm} -vs- \tilde{J} obtained from “collapsing” the isotherms with $J > J_c(T, H)$. The temperature increment δT between successive curves over the critical regime (indicated by the arrows) in (a) is 0.06 K and that in (b) is 0.08 K.

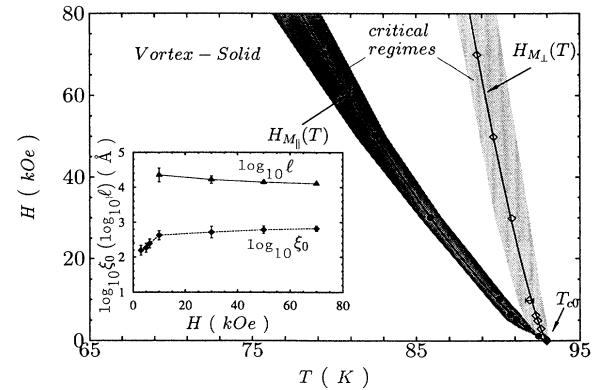


FIG. 2. The anisotropic vortex-solid melting transition lines $H_{M\parallel c}(T)$ and $H_{M\perp c}(T)$ obtained from the critical scaling analysis. The shaded areas denote the critical regimes of the two melting lines. The inset shows the log values (in Å) of the correlation length ($\log_{10} \xi_0$) and the vortex mean free path ($\log_{10} \ell$) as a function of the magnetic field (H).

rupted by the twin boundaries (or by the edge of the screw dislocations) whenever $\xi \sim l$, where l is a "vortex mean free path" comparable to the average twin boundary separation (or the diameter of a typical screw dislocation). Consequently, for constant T and H there is a characteristic current density $J_l(T, H)$ defined by the relation $\xi(T, H, J_l) = l$, such that for $J < J_l$ the vortex dislocation loops are pinned by the twin boundaries, and the critical scaling of the E -vs- J isotherms breaks down. From Eqs. (1) and (2) we note that $J_l(T_M) = [(k_B T_M)/(l^2 \Phi_0)]$ is independent of the exact functional form of $f(x)$, and therefore l can be determined if $J_l(T, H)$ is known. Experimentally, for a given temperature and in a constant magnetic field, J_l can be measured by identifying the current density below which the critical scaling expression in Eq. (3) breaks down. In Fig. 3 we show the temperature dependence of J_T and J_l for $H = 30$ kOe by using Eqs. (1) and (2), and the following experimental parameters determined from the data in Fig. 1(b): $T_M = 85.98$ K, $\nu = \frac{2}{3}$, and $z = 3$. The J_l curve in Fig. 3 is drawn by the simple choice $f(x) = 1/\sqrt{1+x}$, and the dots are the measured values of J_l near T_M . These lead to $l \approx 2 \mu\text{m}$, in good agreement with the twin boundary separation of our single crystal. We note that l varies from 2.2 to 1.3 μm for magnetic fields from 1 to 70 kOe (see Fig. 2). The slight decrease of l with the increasing magnetic field may be attributed to the increasing range of vortex-twin interaction which reduces the vortex mean free path.¹⁶ Thus, the presence of J_l is a natural consequence of the finite-size effect, not to be mistaken as the hint of another phase transition.²²

Another self-consistent way of demonstrating the pinning effects is to measure the Ohmic magnetoresistivity (ρ) versus T with a small current density $J \ll J_T$, and then to identify a temperature interval ΔT near T_M where the resistivity critical scaling relation [$\rho \sim (T - T_M)^{\nu(z-d+2)}$] (Ref. 3) breaks down. Here ΔT is obtained by asserting $\xi(T, H, J) = l$ at constant J and H , so

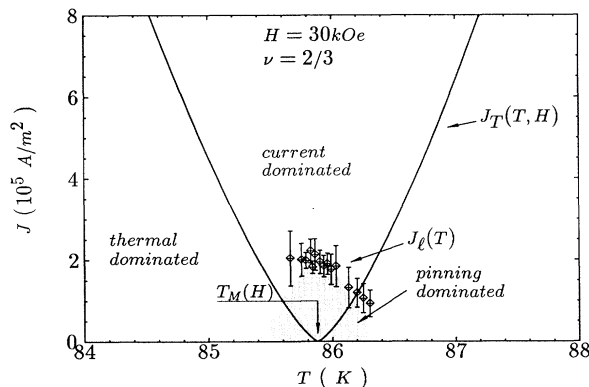


FIG. 3. The current density (J) vs temperature (T) diagram for $H = 30$ kOe. The solid curve shows the characteristic current density $J_T(T, H)$ which separates the current-dominated regime from the thermal-dominated regime. The dashed curve shows the effective "depinning" current density $J_l(T, H)$. The dots are the experimental J_l values obtained from analyzing the E -vs- J isotherms.

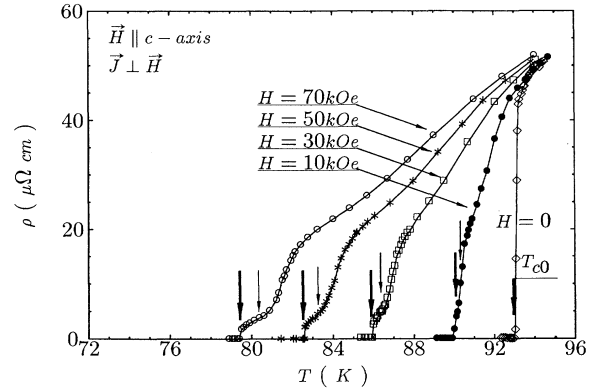


FIG. 4. The Ohmic ρ -vs- T curves at constant magnetic fields for $\mathbf{H} \parallel c$, and $H = 0, 10, 30, 50$, and 70 kOe. The melting temperatures $T_M(H)$ obtained from the critical scaling analysis are indicated by the bold arrows, and the crossover temperatures $T_x(H)$ (see the text) are indicated by the light arrows.

that $\Delta T \equiv T_M(\xi_0/l)^{1/\nu}$ [see Eq. (1)]. Note that ΔT increases with the increasing H (larger ξ_0) and the decreasing vortex mean free path (smaller l). In Fig. 4 the melting temperatures $T_M(H)$ for $\mathbf{H} \parallel c$ axis are indicated by the arrows on the $\rho(T, H)$ -vs- T plot, and so are the crossover temperatures $T_x(H)$, defined as $T_x \equiv T_M + \Delta T$. We find good agreement between the $T_x(H)$ values and the temperatures where distinct changes in the resistivity occur. It should be noted that the resistivity "kink" near T_x is only visible for twinned crystals^{16,23} with a well-defined vortex mean free path (l). The "kink" disappears in inhomogeneous samples (such as epitaxial films and irradiated single crystals¹⁶) with a broad distribution of l values, also in untwinned single crystals where l is practically the size of the sample and $l \gg \xi_0$, $\Delta T \rightarrow 0$.

We have shown in separate publications^{14,15} the experimental results of both the amplitudes $\rho(T, H, \omega)$ and the phases $\phi(T, H, \omega)$ of the ac resistivity in Y-Ba-Cu-O single crystals. We find that critical scaling relations also apply to the ac resistivity data, which yield critical exponents ($\nu \approx \frac{2}{3}$ and $z \approx 3.0$) and a melting line $H_M(T)$ consistent with those obtained from the dc measurements. In the following we only demonstrate the procedure used to obtain the vortex critical relaxation rate $\omega_T(T, H)$ from the universal functions $\bar{\rho}_{\pm}(\bar{\omega})$.^{14,15} Define $\bar{\rho}(\bar{\omega}) \equiv [(E/J)|1 - (T/T_M)|^{\nu(d-2-z)}]$, $\bar{\omega} \equiv (\omega/\omega_c)|1 - (T/T_M)|^{-\nu z}$, and $\omega_T(T, H) = \omega_c(H)|1 - (T/T_M)|^{\nu z}$. The temperature-independent coefficient of the critical-relaxation rate, $\omega_c(H)$, can be obtained from knowing that $\bar{\rho}_{+}(\bar{\omega}) \approx \bar{\rho}_0$ for $\bar{\omega} \rightarrow 0$ and $\bar{\rho}_{+}(\bar{\omega}) = \bar{\rho}_0 \bar{\omega}^{[1-(1/z)]}$ for $\bar{\omega} \rightarrow \infty$.^{13,15} In Fig. 5 we show the $\omega_c(H)$ values determined directly from $\bar{\rho}_{+}$. We note that $\omega_c \approx 10^{10} - 10^{12}$ Hz for $H = 1 \rightarrow 70$ kOe, with a maximum near 30 kOe. The physical meaning of ω_c is consistent with the temperature-independent coefficient of the thermal relaxation frequency (Γ_1) calculated by Brandt.⁷

In Ref. 11 the critical exponents of a heavily twinned Y-Ba-Cu-O single crystal (with twin boundary separation $< 10^3$ Å and $T_{c0} = 88$ K) were estimated by applying small current densities ($10^2 - 10^4$ A/m²) to measure the

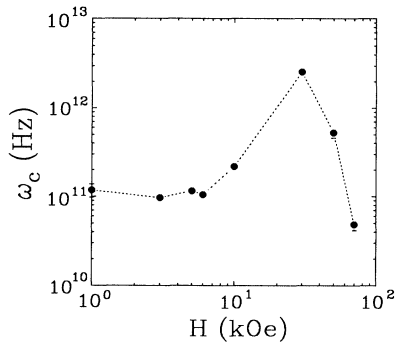


FIG. 5. The temperature-dependent coefficient of the critical relaxation rate, $\omega_c(H)$ (in Hz), is shown as a function of the magnetic field (H). The values of $\omega_c(H)$ are obtained from the data in Ref. 14.

Ohmic resistivity near the “vortex-glass” transition temperature T_G . Using the experimental parameters given in Ref. 11, we find that their applied current densities were insufficient to overcome the twin boundary pinning because $J \ll J_l$. Therefore it is not surprising to find that the data in Ref. 11 do not follow the universal scaling relation in Eq. (3), and that large errors exist in the estimated critical exponents ($\nu=2\pm 1$) and ($z=3.4\pm 1.5$). Similarly, in Ref. 10 the high density of screw dislocations ($10^9-10^{10} \text{ cm}^{-2}$) (Ref. 21) in Y-Ba-Cu-O epitaxial films not only severely limits the current range for the critical scaling (the corresponding J_l becomes 10^6-10^7 A/m^2 , see Fig. 3), but also reduces the number of correlated vortices to $< \sim 10$ in fields up to 40 kOe. Furthermore, the

critical regime estimated by Ref. 10 for $H=40$ kOe is about 12 K, not only far greater than that obtained by using the Ginzburg criterion²⁰ but also strongly overlapping the critical regime of $H_{c2}(T)$, thereby casting large uncertainties on the estimated critical exponents.

Finally, we note that the same ν and z values have also been obtained from the E -vs- J measurements on proton irradiated Y-Ba-Cu-O single crystals,¹⁶ lending additional strong support for the universality of the vortex-solid melting transition. The dynamic exponent $z \approx 3$ obtained from our investigations is significantly smaller than that ($z=4$) obtained by the mean-field calculations of a vortex-glass model.¹⁷ Further theoretical work appears necessary to account for the experimental value $z \approx 3$.

In summary, we have determined the following physical parameters associated with the second-order vortex-solid melting transition in Y-Ba-Cu-O single crystals: the static exponents $\nu \approx \frac{2}{3}$, the dynamic exponent $z \approx 3$, the zero-field critical exponent $\nu_0 \approx \frac{2}{3}$, as well as the vortex-correlation length (ξ_0) and the critical-relaxation rate (ω_c). The critical exponents and the vortex transport functions are shown to be truly *universal*, independent of the experimental technique, point-defect density in the sample, and the magnitude and orientation of the applied dc magnetic field.

This work was jointly supported by the ONR Grant No. N00014-91-J-1556, NASA/OAET, IBM, and the Alfred P. Sloan Foundation. The authors thank Professor M. C. Cross for stimulating discussions, and C. M. Garland for taking the reflecting-light micrographs.

¹D. R. Nelson and H. S. Seung, Phys. Rev. B **39**, 9153 (1989).

²M. C. Marchetti and D. R. Nelson, Phys. Rev. B **41**, 1910 (1990).

³D. S. Fisher, M. P. A. Fisher, and D. Huse, Phys. Rev. B **43**, 130 (1991).

⁴A. Houghton, R. A. Pelcovits, and A. Sudbø, Phys. Rev. B **40**, 6763 (1989).

⁵N.-C. Yeh, Phys. Rev. B **40**, 4566 (1989); **42**, 4850 (1990); **43**, 523 (1991).

⁶P. H. Kes *et al.*, Supercond. Sci. Technol. **1**, 242 (1989).

⁷E. H. Brandt, Int. J. Mod. Phys. B **5**, 751 (1992); Physica C **162**, 1167 (1989).

⁸E. Zeldov *et al.*, Phys. Rev. Lett. **62**, 3093 (1989); S. N. Copersmith *et al.*, *ibid.* **64**, 2585 (1990).

⁹H. Safar *et al.*, Phys. Rev. Lett. **69**, 824 (1992).

¹⁰R. H. Koch *et al.*, Phys. Rev. Lett. **63**, 1511 (1989); **64**, 2586 (1990); H. K. Olsson *et al.*, *ibid.* **66**, 2661 (1991).

¹¹P. L. Gammel *et al.*, Phys. Rev. Lett. **66**, 953 (1991).

¹²N.-C. Yeh *et al.*, Phys. Rev. B **45**, 5654 (1992). In this paper $\nu \approx 0.9$ and $z \approx 2.0$ for Y-Ba-Cu-O single crystals in fields up to 6 kOe were obtained by indiscriminately including the E -vs- J isotherms over a broad temperature range (up to T_{c0}),

and are probably affected by crossover effects to the mean-field $H_{c2}(T)$. By excluding the isotherms outside the critical regime, the same critical exponents $\nu \approx \frac{2}{3}$ and $z \approx 3$ can be obtained from the previously published data.

¹³N.-C. Yeh, W. Jiang, D. S. Reed, A. Gupta, F. Holtzberg, and A. Kussumal, Phys. Rev. B **45**, 5710 (1992).

¹⁴D. S. Reed, N.-C. Yeh, W. Jiang, U. Kriplani, and F. Holtzberg, following paper, Phys. Rev. B **47**, 6150 (1993).

¹⁵N.-C. Yeh *et al.*, Mat. Res. Soc. Sym. Proc. **275**, 169 (1992).

¹⁶W. Jiang *et al.*, Phys. Rev. B (to be published); W. Jiang *et al.*, Mat. Res. Soc. Sym. Proc. **275**, 789 (1992).

¹⁷A. T. Dorsey, M. Huang, and M. P. A. Fisher, Phys. Rev. B **45**, 523 (1992); A. T. Dorsey, *ibid.* **43**, 7575 (1991).

¹⁸We thank Professor M. C. Cross for directing us to this point.

¹⁹P. C. Hohenberg and B. I. Halperin, Rev. Mod. Phys. **49**, 435 (1977).

²⁰U. Welp *et al.*, Phys. Rev. Lett. **67**, 3180 (1991).

²¹Ch. Gerber *et al.*, Nature **350**, 279 (1991); M. Hawley *et al.*, Science **251**, 1587 (1991).

²²T. Worthington *et al.*, Phys. Rev. B **46**, 11 854 (1992).

²³W. K. Kwok *et al.*, Phys. Rev. Lett. **64**, 966 (1990).

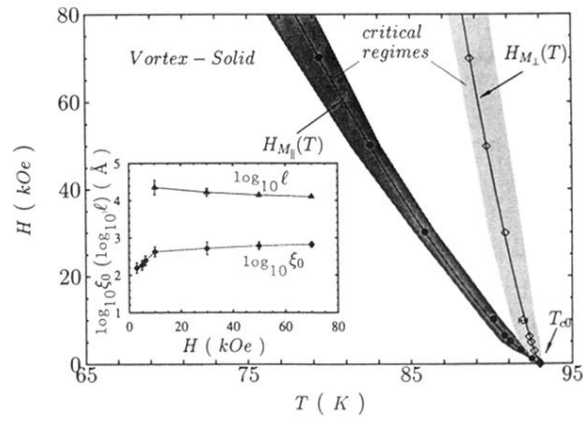


FIG. 2. The anisotropic vortex-solid melting transition lines $H_{M_{||c}}(T)$ and $H_{M_{\perp c}}(T)$ obtained from the critical scaling analysis. The shaded areas denote the critical regimes of the two melting lines. The inset shows the log values (in Å) of the correlation length ($\log_{10} \xi_0$) and the vortex mean free path ($\log_{10} \ell$) as a function of the magnetic field (H).